Empirical Modeling and Analysis of Water-to-Air Optical Wireless Communication Channels

Pooya Nabavi[1], A. F. M. Saniul Haq[2], and Murat Yuksel[1,2]
[1]Electrical and Computer Engineering, University of Central Florida, Orlando, FL USA 32816
[2]College of Optics and Photonics, University of Central Florida, Orlando, FL USA 32816
pooya.nabavi@knights.ucf.edu, saniul.haq@knights.ucf.edu, murat.yuksel@ucf.edu

***Abstract*—Underwater optical wireless communication (UOWC) is attracting significant attention due to global climate monitoring, military applications, and exploration to study marine biology. Optical wireless communication (OWC) can provide the benefits of higher transmission data rate and bandwidth by using unlicensed bandwidth and light-weight transceivers having low power requirements. However, OWC suffers from many limitations such as absorption, scattering, and turbulence, which become harder when the channel includes a water-to-air (W2A) interface. In this paper, we focus on the modeling impulse response of a W2A-OWC channel under different turbulent water surface conditions. We empirically evaluate the statistical behavior of the channel and show fits to probabilistic distributions to understand the nature of the W2A-OWC channels.**

***Index Terms*—Turbulence, Water-to-Air Optical Wireless Communications, Statistical Distribution, Channel Modeling.**

I. Introduction

The light was the first medium of communication since the dawn of civilization, for instance, light beacon was used for military application by Chinese soldiers in around 1,000 BC and the Romans used a polished surface to reflect sunlight to send messages to distant locations. Alexander Graham Bell invented a wireless telephone system in 1880, also known as "photophone", which used reflected sunlight from a vibrating mirror as a transmission medium. With the advancement of technology and increased data volume, another wireless communication technology emerged which uses radio frequency (RF). RF communication has numerous advantages, such as reliability, non-line-of-sight (NLOS) operation, and omnidirectionality. Recently, optical wireless communication (OWC) is grabbing attention due to the spike in data demands, requirement of high bandwidth and data rate, and security of communication channels. Even though OWC channel provides low-power and ultra-high data transmission rates than legacy RF channels, it suffers from various challenges such as absorption and scattering effect, the need for acquisition and maintenance of the line-of-sight (LOS), and moderate link ranges [1]. In the last couple of decades, with ever-changing global climate, ocean exploration and research have become one of the most widely investigated research topics.

Underwater wireless communication (UWC) opened up a tremendous opportunity for researchers to explore and acquire data from deep ocean remotely and safely. UWC technology can be realized by utilizing one of the three existing wireless carriers, i.e., acoustic waves, RF waves, and optical waves. Acoustic waves provide long communication range, but their low transmission rate, high latency, Doppler spread, and potential threat to marine life ultimately limit effective bandwidth and make it difficult to meet researchers' need. RF waves give quite a few benefits such as loose pointing requirements, moderately high data transmission rate, and tolerance to turbid water. However, RF wavelength is very lossy in seawater, hence it can provide link range up to 10 m only [2]. Optical waves, on the other hand, provide very high bandwidth, high transmission rate, low latency, and low power solution, but their communication range too is affected by other factors like scattering and dispersion [3]. But due to relatively low absorption in the visible light spectrum and low power budget for attaining relatively longer ranges of communication, underwater optical wireless communication (UOWC) has been a key focus in the last decade for space to underwater communication.

In water-to-air optical wireless communication (W2A-OWC) channels, three usual adverse factors influencing the diffusion of the propagating optical signals are absorption, scattering, and turbulence, which, respectively, result in signal attenuation, inter-symbol interference (ISI), and signal fading. More importantly, a fourth factor that imposes significantly more adverse effects on the quality of the channel between the receiver located in the free space and the underwater transmitter is the largely unpredictable changes at the air-sea interface caused by the sea waves with random and sometimes non-random patterns. These physical aquatic waves usually prevent direct communication between the transmitter and receiver, which necessitates the need for a communication repeater (which are typically floating buoys [4]) at the air-sea interface, imposing a risk to secure communications in most applications.

In this paper, we model the impulse response of a W2A-OWC channels via rigorous empirical experiments in order to factor in the effects of the random and non-random wave patterns existing at the water surface. These cause the propagating photons to experience an unpredictable path deviation beyond the detrimental absorption and scattering effects resulted by abundant dissolved or unsolved particles existing in both air and water mediums. As a result of these undesired effects, photons will reach the receiver after multiple scatters and experience different emission times in the channel. This increases signal time spread which in turn leads

978-1-7281-2373-8/19/$31.00 ©2019 IEEE

to ISI and increased fading. Finally, we model the channel impulse response by fitting to a random process and study the relationship between the statistics of the impulse response and the specific artificially generated aquatic surface wave patterns.

II. Background and Literature

In this section, we will discuss the development of OWC in the area of free-space and underwater communication. We will also discuss briefly the challenges of OWC between aerial nodes to underwater nodes and already proposed works to mitigate those challenges.

A. Free-Space-Optical Communication

Apart from high bandwidth and data transmission rate, free-space-optical (FSO) communication has many beneficial properties, i.e., low power-per-bit, small form factor, and ease of maintenance. As the number of mobile users is on the rise, FSO links are gaining more interest recently to meet the high data demand. Where RF carrier is bandwidth limited and restricted, FSO spectrum provides higher bandwidth free of licensing costs.

Outdoor FSO systems can be classified into two categories: Terrestrial and space links. These two broad categories include building-to-building, satellite-to-ground, satellite-to-UAV (unmanned aerial vehicles or balloons), and satellite-to-satellite communication [5]. Several experimental demonstrations of such FSO communication links are reported in the last two decades. NASA reported one such ground-to-satellite link, named Ground/Orbital Lasercomm Demonstration (GOLD), using GaAs laser with 1.024 Mbps data transmission rate [6]. Ortiz *et. al.* reported an UAV-to-ground FSO link with 2.5 Gbps using 200 mW laser diode [7]. A Gbps FSO link for building-to-building communication is reported by Fahs *et. al.* having 72 m link range [8]. They implemented the system using vertical cavity surface emitting lasers (VCSEL) and avalanche photo diodes (APD) in the visible spectrum.

B. Underwater Optical Wireless Communication

A major portion of the preliminary underwater communication literature covers the advancement of technology using acoustic waves, but UOWC grabbed significant attention in the last decade. Johnson *et. al.* summarized the extent of underwater light absorption and scattering models and how they might impact the underwater communication system [9]. He evaluated which wavelengths will be optimum to choose for UOWC systems for various type of waters. Over years UOWC became more attractive to researchers as it can exceed Gbps data rates and several experimental studies have been carried out to support the theoretical calculations [10], [11]. Gabriel *et. al.* reported an UOWC system implemented using 532 nm LED as a transmitter and Si APD as a receiver to achieve 1 Gbps over 20 m link [12].

C. Water-to-Air (W2A) Optical Wireless Communication

Our goal is to establish a communication link from an aerial platform to a submerged vehicle. This type of communication link technology is still emerging and under-explored. One of the major challenges for the W2A-OWC link is the air-water interface, which reflects and scatters signals and introduces a loss component that can over-power absorption loss. Even though RF waves have a relatively smooth transition at air-water boundaries, they experience very high absorption in sea-water, and hence, result in low communication range [1]. Darlis *et. al.* reported shore-to-undersea visible light communication, where the signal from a lighthouse is transmitted to an underwater platform through a buoy (relay) at the interface [4], but that defeats the purpose of security of the submerged platform. The effects of wind induced surface wave perturbations on optical propagation for air to underwater FSO are explored by Alharbi *et. al.* [13]. However, they focused on surface wave mapping rather than optical communication channel modeling. Chen *et. al.* experimentally demonstrated an air-water OWC system [14], however, they carried out the experiments with a controlled and static air-water interface under good pointing accuracy. In this paper, we evaluate the W2A-OWC channel through a number of empirical experiments with artificially generated random and non-random waves.

III. Channel and System Model

As briefly discussed in the previous section, a number of factors can cause problems in establishing a reliable optical communication link in W2A-OWC channels. Fading is the most critical factor in this regard, which drastically attenuates the data-carrying optical signal as it propagates towards the receiver. In this study, we investigate the possibility of creating a reliable direct communication link between an optical transmitter and receiver by examining the most adverse factor in these channels, i.e. the aquatic surface waves at the interface of two different mediums that cause optical irradiation fluctuations. In an optical link, irradiance variations, at the receiver, give rise to both fading losses and erasure errors during communications. In order to study these impairments, we have implemented a series of empirical experiments to numerically measure the temporal fluctuations of optical irradiance and its statistics which are solely resulted by the unsettling interface between the cross-section of the water and free space mediums and study the corresponding channels' delay spread and its impulse response. The next few subsections will better explain our evaluation metrics and more importantly the features of our experiments.

A. Irradiance Probability Distribution Function

Optical turbulence effects due to internal scattering existing in homogeneous channels were extensively studied in the literature and numerous distribution models (e.g., Lognormal and negative exponential models) are developed in order to predict specific turbulence conditions, such as weak turbulence for Lognormal model and very strong turbulence (saturate regime) for negative exponential model [15]. In this section, we overview the statistical distributions to model the statistical behavior of impulse response of the W2A-OWC channels. Each statistical distribution contains a set of parameters which can be obtained such that they simultaneously satisfy two essential criteria. The first criteria is the fading normalization equality which means that the fading coefficient is normalized

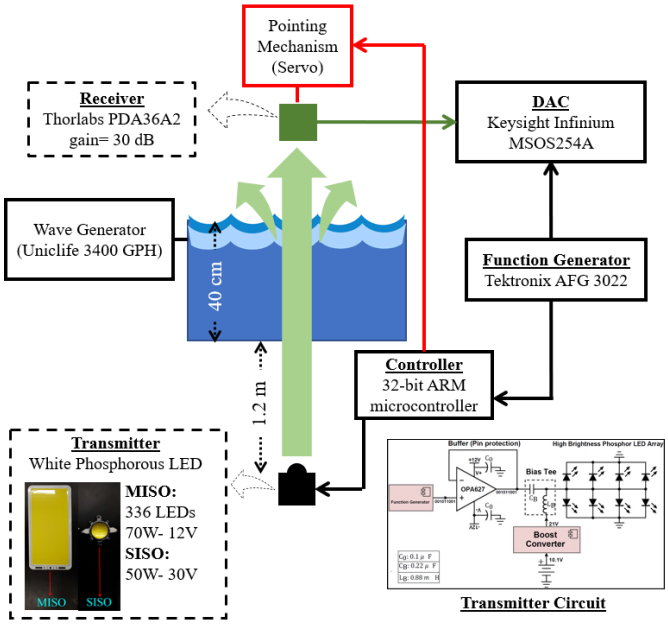

Fig. 1. Experimental setup for W2A-OWC link.

to emphasize that it neither amplifies nor attenuates the average received power. To do so in our experiments, we normalize the received voltage vector from each channel realization, corresponding to the received optical power from a specific wave pattern at each scenario, to its mean to make sure that the mean of the new vector is equal to one. The second criteria that we optimize is the distribution parameters such that they result into the best fit to the experimental data.

B. The Distribution Functions Under Consideration

1) Birnbaum-Saunders Distribution: Motivated by problems of vibration in commercial aircrafts that cause fatigue in materials, Birnbaum and Saunders (1969) introduced a probability distribution that describes lifetimes of specimens exposed to fatigue due to cyclic stress[1]. The Birnbaum-Saunders (B-S) model is based on a physical argument of cumulative damage that produces fatigue in materials, considering the number of cycles under stress needed to force a crack extension due to fatigue to grow beyond a threshold, provoking the failure of the material. The B-S distribution is expressed as:

$$f_X(x) = \frac{\sqrt{\frac{x-\mu}{\beta}} + \sqrt{\frac{\beta}{x-\mu}}}{2\gamma(x-\mu)} \phi\left(\frac{\sqrt{\frac{x-\mu}{\beta}} - \sqrt{\frac{\beta}{x-\mu}}}{\gamma}\right), x > \mu \quad (1)$$

where $\gamma > 0$ is the shape parameter, μ is the location parameter, $\beta > 0$ is the scale parameter, and $\phi(x) = \frac{e^{-\frac{x^2}{2}}}{\sqrt{2\pi}}$ is the probability density function (PDF) of the standard Normal distribution.

2) Lognormal Distribution: The Lognormal distribution is mainly used in the UOWC literature [2] to describe the fluctuations induced by weak underwater turbulence, characterized by $\sigma_I^2 < 1$. The PDF of Lognormal distribution is given by:

[1]As we will observe in the next section, this distribution can model W2A-OWC channel's impulse response at the presence of random surface waves, with the highest goodness of fit in comparison with other existing distributions.

$$f_X(x) = \frac{1}{2x\sqrt{2\pi\sigma_x^2}} \exp\left(-\frac{(\ln(x) - 2\mu_X)^2}{8\sigma_X^2}\right) \quad (2)$$

where μ_X and σ_X^2 are respectively the mean and variance of the Gaussian-distributed fading log-amplitude factor defined as $X = \frac{1}{2}\ln(x)$ [15].

IV. Experimental Setup

The experimental setup of the optical receiver and transmitter employed in the W2A-OWC channel is demonstrated in Fig. 1. As shown, the entire receiver structure is assembled on a servomotor, using which the initial calibration of the receiver can be carried out in order to accurately establish a LOS between the transmitter and receiver. A micro-controller was used to control the servomotor. As a result, the entire mechanism allows creating an accurate LOS link between the transmitter and the receiver of the optical system. To this end, prior to starting the communication, the receiver makes a 180-degree swing while simultaneously monitoring the receiver signal-to-noise ratio (SNR). Once the spatial scanning successfully is completed, the servomotor stops rotating and aligns the receiver to the angular position corresponding to highest SNR.

Various scenarios and sets of experiments are performed. In the first scenario, the effects of different aquatic surface wave patterns at the air-water cross-section on the quality of received signals was evaluated and studied. To this end, the eye diagram was plotted for the received signal at a transmission bit rate of 100 Kbps for three cases of surface waves: pulse, random, and none. For achieving this purpose, we constructed data eye diagram from a digital waveform present in the output of the photodetector in the receiver side. By folding the parts of the waveform corresponding to each individual bit into a single graph with signal amplitude on the vertical axis and time on the horizontal axis. By repeating this construction over many samples of the waveform, the resultant graph represents the average statistics of the signal and resembles an eye. The eye-opening corresponds to one-bit period and is typically called the Unit Interval (UI) width of the eye diagram.

In the second scenario, the channel impulse response was evaluated and estimated to calculate the delay spread of the W2A-OWC channel. In this scenario, Single-Input Single-Output (SISO) and Multiple-Input Single-Output (MISO) communication structures were considered for three cases of aquatic pulse, random and no surface waves. A full-1 signal (always-on optical signal) is sent by utilizing the white phosphorous light emitting diodes in the transmitter, and the corresponding voltage signal is stored and received from the output of the transimpedance amplifier in the receiver. This signal is in proportion to the luminous intensity radiated on the photodiode window. Finally, by normalizing the received signal (to have an average value equal to one) and plotting its corresponding histogram, the statistical distribution of the impulse response of the studied channel under the aforementioned conditions is obtained. Moreover, we have calculated

the root mean square (RMS) delay spread for the W2A-OWC channel in using [11]:

$$\tau_{\mathrm{RMS},i} = \sqrt{\frac{\int_{-\infty}^{\infty}(t-\tau_i)^2 h_i^2(t)\mathrm{d}t}{\int_{-\infty}^{\infty} h_i^2(t)\mathrm{d}t}}, \quad i = 1,\ 2,\ 3 \qquad (3)$$

where $h_i(t)$ is the estimated channel impulse response for three cases of pulse waves ($h_1(t)$), random waves ($h_2(t)$), and no waves ($h_3(t)$) at the W2A interface. τ_i is the mean delay due to non-LOS paths and given by $\tau_i = \int_{-\infty}^{\infty} h_i^2(t)t\mathrm{d}t \Big/ \int_{-\infty}^{\infty} h_i^2(t)\mathrm{d}t$, i=1,2,3. Using Eq. (3) in a SISO communication structure, we empirically measured the effective delay spread in the W2A-OWC channel as $\tau_{\mathrm{RMS},1}$=0.2 μs, $\tau_{\mathrm{RMS},2}$=3.1 μs and $\tau_{\mathrm{RMS},3}$=2.75 μs for no wave, pulse waves and random waves, respectively.

V. Numerical Results and Discussion

The eye diagrams in Fig. 2(a)-(c) provide instant visual data that can be used to check the overall system's signal integrity in presence of different wave patterns in the W2A channel. We installed an aquatic wave generator on the body of the container to generate the desired aquatic wave patterns at interface of the water and air mediums. Furthermore, we used a frequency controller to generate and apply the desired speed and pattern in the aquatic waves. As shown, presence of aquatic waves at the interface of two mediums, regardless of the pattern of the wave, causes severe distortion and closer eyes due to the considerable increase in the ISI.

A. SNR Observed at the Receiver

For accurate characterization of the W2A interface, we used ultrasonic sensors in presence of different water wave patterns. To this end, the ultrasonic sensor installed in the optical system receiver transmits an acoustic pulse at 1 ms time intervals to the transmitter. Given the speed of sound, the distance of the receiver in air from the disturbed water can then be obtained in real time by measuring the elapsed time between the emitted signal and its received reflection from the water surface. As demonstrated in Fig. 2(d), in the absence of water waves, the distance between the receiver and the interface of the two mediums is constant over time, allowing the optical power of the received signal to experience a lower level of distortion. The reason can be explained by the fact that most emitted photons from the transmitter maintain their direct path and reach the receiver with a negligible time delay of 0.2 μs in the impulse response of the optical channel, which is caused by the collision of photons with the particles floating inside the water and air. Moreover, the channel loss also reduces in this case, which results in achieving an SNR ratio of 36 dB in the receiver of the optical system and a highly reliable communication channel.

We observe that the aquatic waves cause notable reduction in the SNR of the W2A channel. As shown in Fig. 2(e), we measured the distance between the receiver and the W2A interface while generating pulse wave patterns in the water surface. As shown, this spatial distance between the receiver and surface is continuously changing in a periodic manner with a period of 0.9 ms. In this case, the emitted photons are scattered as they collide with the severely disturbed water surface and reach the optical receiver with different time delays due to multi-path propagation. As a result, a significant time delay is observed in the channel impulse response as we will show next. Moreover, some of the emitted photons never reach the receiver surface, consequently increasing the channel loss and reducing the SNR to 34 dB. In Fig. 2(f), we make the same measurement in the presence of random waves at the water surface. These random waves further intensify the loss in the channel, which consequently reduces the SNR to 26 dB.

B. Channel Impulse Response

The output voltage histogram of a photodetector in the optical receiver is demonstrated in Fig. 2(g)-(i), to empirically model the W2A-OWC channel and evaluate the statistical behavior of the impulse response. As shown in Fig. 2(g), in the absence of aquatic waves, the impulse response of the channel is composed of multiple Dirac functions which are due to a negligible multi-path effect existing in static water surface. As a result, the delay spread of the impulse response is measured to be 0.2 μs, which is negligibly small.

We observe that pulse waves cause a significant delay spread on the W2A-OWC channel. As shown in Fig. 2(h), the PDF of the channel impulse response was experimentally modeled using the histogram of the received voltage in presence of pulse waves. As seen in Fig. 2(j), the persistent periodically oscillating waves increase the delay spread, causing the impulse response to lose its ideal impulse-like and deterministic behavior. In addition, after evaluating different probability distributions, we found that the B-S distribution achieves the highest goodness of fit compared to the other closed-form distribution functions such as Lognormal distribution.

Similar to the pulse waves, random surface waves cause scattering of the transmitted photons and deviation from their direct LOS path from the transmitter as seen in Fig. 2(i). As shown in Fig. 2(i), the Lognormal (green curve) and the B-S (red curve) distributions can well predict the statistical behavior of the channel impulse response in the presence of random surface waves. However, the latter is preferred since, in addition to having a higher goodness of fit, the B-S distribution more accurately predicts the tail behavior of the impulse response in both cases of pulse and random waves, as depicted in the Normal probability plots[2] at Fig. 2(k) and 2(l). Therefore, the B-S PDF is one of the most appropriate candidates to statistically model the channel impulse response in the presence of aquatic waves at the W2A interface of W2A-OWC channels which also interestingly resembles the dynamics of the crack-induced failure of materials under cyclic stress.

[2]Note that a Normal probability plot compares the empirical distribution function of a data set with specified theoretical distribution functions, which are Lognormal and B-S in this case. Furthermore, the Normal probability plot magnifies the small and high probability samples, which helps us better see the empirical distribution's tails.

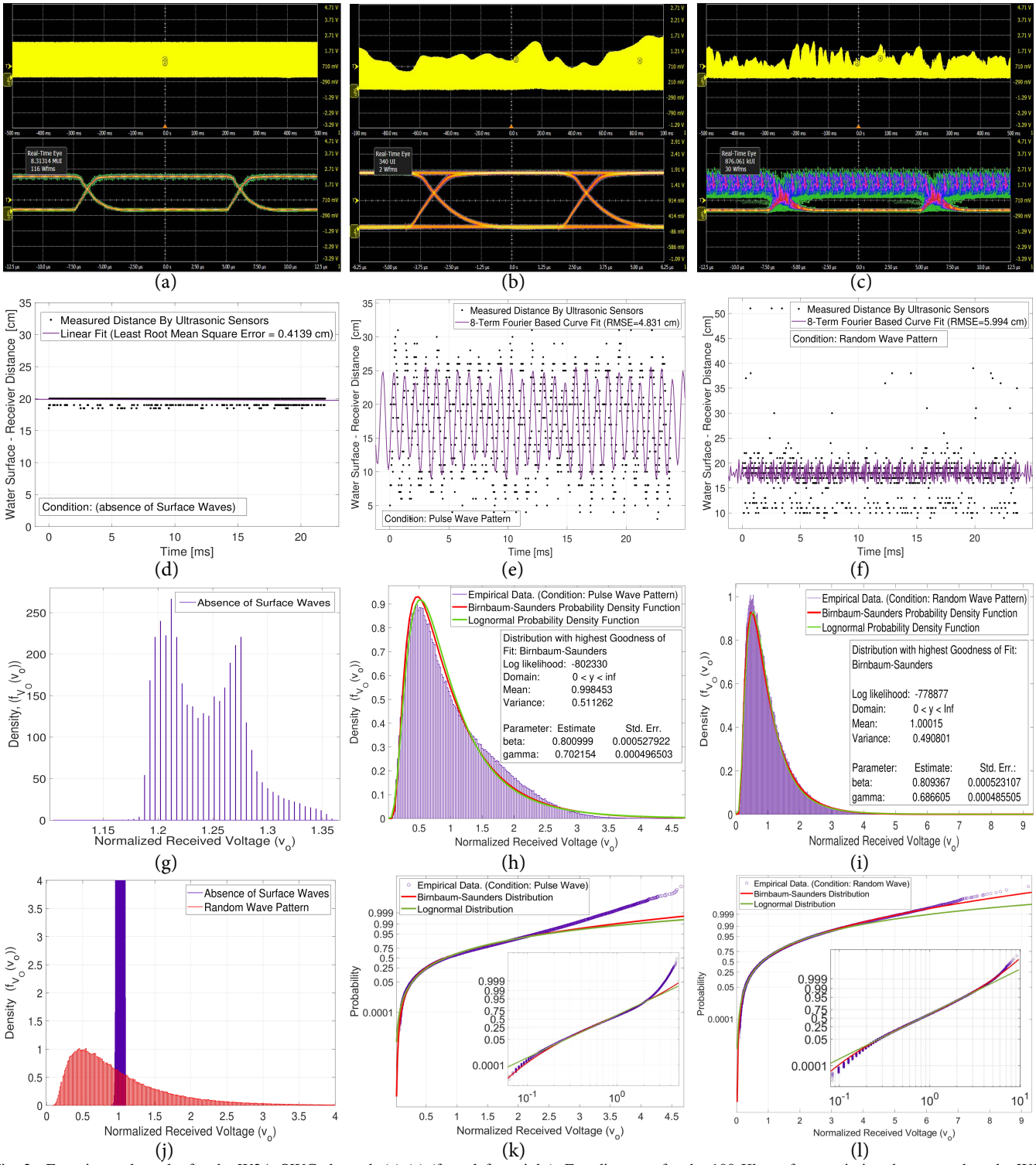

Fig. 2. Experimental results for the W2A-OWC channel: (a)-(c) (from left to right): Eye diagrams for the 100 Kbps of transmission data rate when the W2A interface has no waves, pulse waves, and random waves, respectively, (d)-(f) (from left to right): Ultrasonic surface mapping when the W2A interface has no waves, pulse waves, and random waves, respectively, (g)-(i) (from left to right): Histogram and estimated PDF for the channel impulse response when the W2A interface has no waves, pulse waves, and random waves, respectively, (j) Comparison between impulse response of the channel in both absence and presence of pulse waves in water surface, (k)-(l) (from left to right): The Normal probability plot of the empirically derived impulse response of the channel along with Normal probability plot of the estimated B-S and Lognormal distributions in presence of pulse and random waves, respectively.

As shown in Fig. 2(j), the delay spread of the channel impulse response is simultaneously compared in presence of random aquatic waves and in their absence. As mentioned earlier, these random waves considerably increase the delay spread and consequently the undesirable ISI in the received signal. This, in turn, prevents the receiver from detecting transmitted signals and causes difficulties in establishing a reliable communication link.

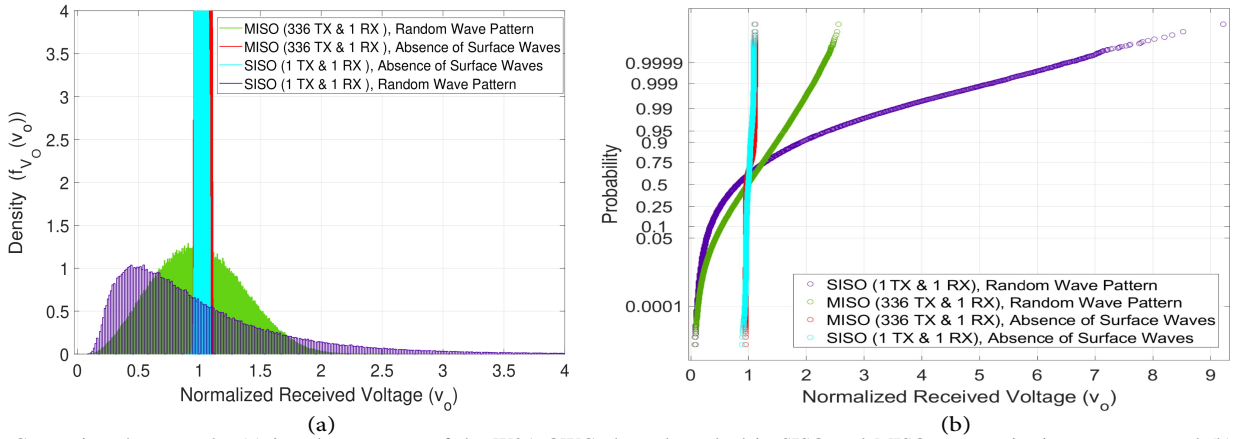

Fig. 3. Comparison between the (a) impulse response of the W2A-OWC channel resulted in SISO and MISO communication structures and (b) Normal probability plot of the impulse response corresponding to no waves, pulse waves, and random waves.

C. Effect of Transmit Diversity

The channel impulse response for SISO and MISO communication structures is compared in Fig. 3 in both presence and absence of random aquatic waves at the water surface. Unlike the SISO structure, a total of 336 transmitters of visible light LEDs were used in the MISO structure. As shown, employing MISO communication structures considerably decreases the delay spread in the channel impulse response from 2.75μs to 2.33μs. This also indicates the usefulness of exploiting transmit diversity to cope with the highly destructive effect of wave-induced ISI in W2A-OWC channels. It is an open issue to explore the optimal transmitter diversity (i.e., the number of transmitters in the sender side) for a W2A-OWC channel with a particular wave pattern.

VI. Conclusions

We conducted a set of experimental tests and investigations to model and evaluate the statistical behavior of the impulse response in W2A-OWC channels. We empirically validated the channel model results through real-time transmission of the data and plotting the eye diagram for the received signal. To this end, we generated different aquatic wave patterns at the intersection of air-water mediums in order to induce scattering turbulence along the propagation path of the emitted photons. The statistical distribution function of the channel impulse response was successfully modeled under different conditions by measuring and receiving the transmitted signals in the receiver of the optical system. Our study revealed that the Birnbaum-Saunders distribution function, with considerably high precision and goodness of fit, was able to predict the statistical behavior of the W2A-OWC channel compared to the other closed-form distribution functions. Further, we observed that pulse-like aquatic waves at the water surface cause a significant delay spread of 3.1 μs along with a considerable decrease in the SNR. In the presence of random aquatic waves, it was concluded that the Birnbaum-Saunders distribution function was still able to predict the statistical behavior of channel impulse response with the highest goodness of fit. Finally, employing MISO communication structures considerably decreased the delay spread in the channel impulse response.

References

[1] Z. Zeng, S. Fu, H. Zhang, Y. Dong, and J. Cheng, "A survey of underwater optical wireless communications," *IEEE communications surveys & tutorials*, vol. 19, no. 1, pp. 204–238, 2017.

[2] H. Kaushal and G. Kaddoum, "Underwater optical wireless communication," *IEEE access*, vol. 4, pp. 1518–1547, 2016.

[3] X. Yi, Z. Li, and Z. Liu, "Underwater optical communication performance for laser beam propagation through weak oceanic turbulence," *Applied Optics*, vol. 54, no. 6, pp. 1273–1278, 2015.

[4] A. R. Darlis, W. A. Cahyadi, and Y.-H. Chung, "Shore-to-undersea visible light communication," *Wireless Personal Communications*, vol. 99, no. 2, pp. 681–694, 2018.

[5] H. Kaushal and G. Kaddoum, "Optical communication in space: Challenges and mitigation techniques," *IEEE communications surveys & tutorials*, vol. 19, no. 1, pp. 57–96, 2017.

[6] K. Wilson, "An overview of the GOLD experiment between the ETS-VI satellite and the table mountain facility," *The Telecommunications and Data Acquisition Progress Report 42-124, Dec 1995*, pp. 8–19, 1996.

[7] G. G. Ortiz, S. Lee, S. P. Monacos, M. W. Wright, and A. Biswas, "Design and development of robust ATP subsystem for the Altair UAV-to-ground lasercomm 2.5-Gbps demonstration," in *Free-Space Laser Communication Technologies XV*, vol. 4975. International Society for Optics and Photonics, 2003, pp. 103–115.

[8] B. Fahs, M. Romanowicz, and M. M. Hella, "A Gbps building-to-building VLC link using standard CMOS avalanche photodiodes," *IEEE Photonics Journal*, vol. 9, no. 6, pp. 1–9, 2017.

[9] L. J. Johnson, "The underwater optical channel," *Dept. Eng., Univ. Warwick, Coventry, UK, Tech. Rep*, 2012.

[10] C. Shen, Y. Guo, X. Sun, G. Liu, K.-T. Ho, T. K. Ng, M.-S. Alouini, and B. S. Ooi, "Going beyond 10-meter, Gbit/s underwater optical wireless communication links based on visible lasers," in *Opto-Electronics and Communications Conference (OECC), 2017*. IEEE, 2017, pp. 1–3.

[11] M. V. Jamali, P. Nabavi, and J. A. Salehi, "MIMO underwater visible light communications: Comprehensive channel study, performance analysis, and multiple-symbol detection," *IEEE Transactions on Vehicular Technology*, vol. 67, no. 9, pp. 8223–8237, Sep. 2018.

[12] C. Gabriel, A. Khalighi, S. Bourennane, P. Léon, and V. Rigaud, "Optical communication system for an underwater wireless sensor network," in *EGU General Assembly Conference Abstracts*, vol. 14, 2012, p. 2685.

[13] O. Alharbi, W. Xia, M. Wang, P. Deng, and T. Kane, "Measuring and modeling the air-sea interface and its impact on FSO systems," in *Laser Communication and Propagation through the Atmosphere and Oceans VII*, vol. 10770, 2018, p. 1077002.

[14] Y. Chen, M. Kong, T. Ali, J. Wang, R. Sarwar, J. Han, C. Guo, B. Sun, N. Deng, and J. Xu, "26 m/5.5 Gbps air-water optical wireless communication based on an OFDM-modulated 520-nm laser diode," *Optics express*, vol. 25, no. 13, pp. 14 760–14 765, 2017.

[15] M. V. Jamali, A. Mirani, A. Parsay, B. Abolhassani, P. Nabavi, A. Chizari, P. Khorramshahi, S. Abdollahramezani, and J. A. Salehi, "Statistical studies of fading in underwater wireless optical channels in the presence of air bubble, temperature, and salinity random variations," *IEEE Transactions on Communications*, vol. 66, no. 10, pp. 4706–4723, Oct 2018.